Time-Varying Coherence Function for Atrial Fibrillation Detection

Jinseok Lee*, *Member, IEEE*, Yunyoung Nam, David D. McManus, and Ki H. Chon, *Senior Member, IEEE*

***Abstract*—We introduce a novel method for the automatic detection of atrial fibrillation (AF) using time-varying coherence functions (TVCF). The TVCF is estimated by the multiplication of two time-varying transfer functions (TVTFs). The two TVTFs are obtained using two adjacent data segments with one data segment as the input signal and the other data segment as the output to produce the first TVTF; the second TVTF is produced by reversing the input and output signals. We found that the resultant TVCF between two adjacent normal sinus rhythm (NSR) segments shows high coherence values (near 1) throughout the entire frequency range. However, if either or both segments partially or fully contain AF, the resultant TVCF is significantly lower than 1. When TVCF was combined with Shannon entropy (SE), we obtained even more accurate AF detection rate of 97.9% for the MIT-BIH atrial fibrillation (AF) database ($n = 23$) with 128 beat segments. The detection algorithm was tested on four databases using 128 beat segments: the MIT-BIH AF database, the MIT-BIH NSR database ($n = 18$), the MIT-BIH Arrhythmia database ($n = 48$), and a clinical 24-h Holter AF database ($n = 25$). Using the receiver operating characteristic curves from the combination of TVCF and SE, we obtained a sensitivity of 98.2% and specificity of 97.7% for the MIT-BIH AF database. For the MIT-BIH NSR database, we found a specificity of 99.7%. For the MIT-BIH Arrhythmia database, the sensitivity and specificity were 91.1% and 89.7%, respectively. For the clinical database (24-h Holter data), the sensitivity and specificity were 92.3% and 93.6%, respectively. We also found that a short segment (12 beats) also provided accurate AF detection for all databases: sensitivity of 94.7% and specificity of 90.4% for the MIT-BIH AF, specificity of 94.4% for the MIT-BIH-NSR, the sensitivity of 92.4% and specificity of 84.1% for the MIT-BIH arrhythmia, and sensitivity of 93.9% and specificity of 84.4% for the clinical database. The advantage of using a short segment is more accurate AF burden calculation as the timing of transitions between NSR and AF are more accurately detected.**

***Index Terms*—Atrial fibrillation (AF), cardiac arrhythmia, ECG, parametric time-frequency spectra, Shannon entropy (SE), short physiological time series, time-varying coherence function, time-varying transfer function.**

Manuscript received April 17, 2013; revised May 20, 2013; accepted May 20, 2013. Date of publication May 22, 2013; date of current version September 14, 2013. This work was supported in part by the office of Naval Research work unit under Grant N00014-08-1-0244. *Asterisk indicates corresponding author.*

*J. Lee is with the Department of Biomedical Engineering, Wonkwang University School of Medicine, Iksan, Jeonbuk, Korea (e-mail: gonasago@wku.ac.kr).

Y. Nam and K. H. Chon are with the Department of Biomedical Engineering, Worcester Polytechnic Institute, Worcester, MA 01609 USA (e-mail: yynams@gmail.com; kichon@wpi.edu).

D. D. McManus is with the Cardiology Division, Departments of Medicine and Quantitative Health Sciences, University of Massachusetts Medical Center, Worcester, MA 01605 USA (e-mail: mcmanus.dave@gmail.com).

Color versions of one or more of the figures in this paper are available online at http://ieeexplore.ieee.org.

Digital Object Identifier 10.1109/TBME.2013.2264721

I. Introduction

ATRIAL fibrillation (AF) is the most common sustained dysrhythmia in the U.S. More than 2.3 million Americans are currently diagnosed, and the prevalence of AF is increasing rapidly with the aging of the U.S. population [1]. Through its association with increased risk for stroke, heart failure, and mortality, AF has a profound impact on the longevity and quality of life of a growing number of people [2], [3]. Although AF treatment strategies are available, a major challenge facing clinicians and researchers is the oftentimes paroxysmal and minimally symptomatic nature of AF, particularly in its early stages. Since even short episodes of AF are associated with adverse health outcomes, there is a pressing need to develop methods for the accurate detection of paroxysmal AF. Such a method would have important clinical applications for use of anticoagulants, antiarrhythmic agents, and ablative therapies to abrogate the effects of AF and its complications. For these reasons, the importance of developing new AF detection technologies has been emphasized [1]–[3].

Many algorithms have been developed to detect AF and can be categorized as being based on 1) P-wave detection or 2) RR interval (RRI) variability [4]–[12]. AF detection based on the absence of electrocardiographic P-waves has not gained wide acceptance because the determination of the P-wave fiducial point localization is challenging, especially for Holter monitoring applications. Indeed, for Holter monitoring, it is difficult to find uncontaminated RRIs due to motion and noise artifacts that can confound accurate P-wave detection. Subsequently, many studies have used the variability of RRI time series instead [8]–[12]. Specifically, the aim is to quantify markedly increased beat-to-beat variability RRI time series in AF. Consequently, most algorithms show higher sensitivity and specificity values than the methods that screen for the absence of P-waves. However, most of these RRI methods are based on comparing the density histogram of the data segment with previously compiled standard density histograms of RR segments during AF using the Kolmogorov–Smirnov test [12]. The main disadvantage of this approach is that it requires storage of large amounts of histogram data and threshold values of various characteristics of AF.

In this paper, we use our previously developed time-varying coherence function (TVCF) approach [13] to discriminate between AF and nonfibrillatory cardiac rhythms. Note that Sarraf *et al*. [14] have used a time-invariant coherence function approach to discriminate between AF and non-AF rhythms with good results. To account for nonstationary dynamics of AF as well as to capture transitions from AF to sinus rhythms, Lovett and Ropella [15] have used a spectrogram approach. However,

the study was not intended for the AF detection; hence its accuracy value is not known. Further, because the spectrogram does not provide the best time and frequency resolution, its ability to find the transition between AF and normal sinus rhythms (NSRs) is not optimal.

In general, the higher time and frequency resolutions offered by the parametric approaches, as compared to nonparametric approaches, are well documented [16]. Hence, our autoregressive moving average (ARMA) model-based TVCF offers higher time and frequency resolutions than do nonparametric approaches. Specifically, an ARMA model-based time-varying transfer function (TVTF) is calculated between two adjacent data segments with one data segment as the input and the other as the output. We then reverse the input and output signals and compute the second TVTF, and then multiply the two TVTFs to obtain the TVCF [13]. Our underlying hypothesis for the use of the TVCF approach is that if the two adjacent segments are NSRs, the resultant TVCF will have values close to one throughout the entire frequency range. However, if either or both segment(s) partially or fully contains AF, the coherence values will dip significantly below one at the time instant AF occurs. Finally, to increase the accuracy of our AF detection, we combined TVCF results with Shannon entropy (SE) as the latter has been shown to be useful for the AF detection [8]. Note a preliminary version of this paper has been reported [32].

II. Methods

A. Databases

We used five databases to test the method on: the MIT-BIH AF, the MIT-BIH NSR, the MIT-BIH Arrhythmia (Arr) [17], a 24-h AF database from The Scottcare Corporation and pre- and postcardioversion clinical trial data from the University of Massachusetts Medical Center (UMMC) to detect AF and NSR, respectively, using an iPhone 4S camera. For all databases, we used RRI series. The MIT-BIH AF database contains 25 ECG recordings in which there are a total of 299 AF episodes. Each ECG recording is approximately 10 h in duration. The data sets 4936 and 5091 were excluded from our study due to incorrect AF annotations. Based on the MIT-BIH AF database ($n = 23$, 1 131 097 beats), threshold values were determined. The MIT-BIH NSR database contains 18 ECG recordings (1 729 629 beats), and the duration of each ECG record is approximately 24 h. The NSR data do not contain AF episodes; hence, they were used for the evaluation of the specificity value of AF detection. The MIT-BIH Arr database consists of 48 half-hour annotated ECG recordings sampled at 360 Hz; 100 series ($n = 23$, 47 891 beats) contain both sinus rhythm and arrhythmias without AF episodes while 200 series ($n = 25$, 64 101 beats) contain AF, various arrhythmias, and sinus rhythm. The clinical AF database consists of 24-h Holter monitor data collected from 25 subjects using ScottCare's RZ153 series recorders. Data were acquired at 180 samples per second with 10-bit resolution. The AF annotation was performed by ScottCare Corporation technicians, and the analysis for R-wave peak detection was done using ScottCare's HolterCare software. The extracted RRIs were then analyzed by the authors using MATLAB 2010a. For the iPhone 4S data collection, 74 patients with AF who presented for electrical cardioversion to the UMMC cardiac electrophysiology laboratory were recruited by trained study personnel. The camera of an iPhone 4S was placed on either the index or middle finger of study participants for 2 min prior to, and again immediately after, cardioversion. Data were recorded in the supine position (to minimize motion artifacts) with spontaneous breathing, with the assistance of a physician. These studies including data analysis were approved by the UMMC Institutional Review Board.

B. Time-Varying Coherence Function

We have previously shown that the TVCF can be obtained by the multiplication of the two time-varying transfer functions [14]. Thus, we will briefly describe the approach. To demonstrate the use of the TVTF in obtaining the TVCF, we first define the TVCF via the nonparametric time-frequency spectra as

$$|\gamma(t,f)|^4 = \frac{|S_{xy}(t,f)|^2}{S_{xx}(t,f)S_{yy}(t,f)} \frac{|S_{yx}(t,f)|^2}{S_{yy}(t,f)S_{xx}(t,f)} \quad (1)$$

where $S_{xy}(t,f)$ and $S_{yx}(t,f)$ represent the time-frequency cross spectrum, and $S_{xx}(t,f)$ and $S_{yy}(t,f)$ represent the auto spectra of the two signals x and y, respectively. Specifically, the first factor in (1) is the coherence function when x is considered as the input and y as the output. Similarly, the second factor in (1) is the coherence function when y is considered as the input and x as the output. For a linear TV system with x as the input and y as the output, the TVTF in terms of time-frequency spectra can be obtained as

$$H_{x\to y}(t,f) = \frac{S_{xy}(t,f)}{S_{xx}(t,f)} \quad (2)$$

where $H_{x\to y}(t,f)$ is the TVTF from the input x to the output y signal. Similarly, for a linear TV system with y as the input and x as the output, the TVTF can be obtained as

$$H_{y\to x}(t,f) = \frac{S_{yx}(t,f)}{S_{yy}(t,f)}. \quad (3)$$

Thus, the time-varying magnitude $|\gamma(t,f)|^2$ is obtained by multiplying the two transfer functions

$$|H_{x\to y}(t,f)\, H_{y\to x}(t,f)|. \quad (4)$$

Given the relationship of (4), a high resolution TVCF can be obtained from ARMA models

$$y(n) = -\sum_{i=1}^{P_1} a(n,i)\, y(n-i) + \sum_{j=0}^{Q_1} b(n,j)\, x(n-j) \quad (5.1)$$

$$x(n) = -\sum_{i=1}^{P_2} \alpha(n,i)\, x(n-i) + \sum_{j=0}^{Q_2} \beta(n,j)\, y(n-j) \quad (5.2)$$

where (5-1) represents *y(n)* as the output and *x(n)* as the input. Similarly, (5-2) represents *x(n)* as the output and *y(n)* as the input. Given the ARMA models of (5), the two transfer functions

of (4) can be obtained as [13]

$$H_{x\to y}\left(n,e^{jw}\right)=\frac{B\left(n,e^{jw}\right)}{A\left(n,e^{jw}\right)}=\frac{\sum_{l=0}^{Q_1}b\left(n,j\right)e^{-jwl}}{1+\sum_{i=1}^{P_1}a\left(n,i\right)e^{-jwi}}$$

$$H_{y\to x}\left(n,e^{jw}\right)=\frac{\beta\left(n,e^{jw}\right)}{\alpha\left(n,e^{jw}\right)}=\frac{\sum_{l=0}^{Q_2}\beta\left(n,j\right)e^{-jwl}}{1+\sum_{i=1}^{P_2}\alpha\left(n,i\right)e^{-jwi}}. \quad (6)$$

Finally, we can obtain the TVCF by multiplying the two transfer functions as described in (6). For the parameter estimation, we can use the time-varying optimal parameter search (TVOPS) criterion [18], which has been shown to be accurate when applied to many diverse physiological signals [19]–[21]. For the physiological signals considered, the TVOPS has been shown to be more accurate than the AIC, minimum description length, and the fast orthogonal search criterion [19]–[21]. For TVOPS, time-varying coefficients are expanded onto a set of basis functions. By expanding each time-varying (TV) coefficient onto a finite set of basis functions, the model order selection criterion of TV systems becomes equivalent to determining model order for time-invariant ARMA. We have previously demonstrated that Legendre polynomials are a good choice for capturing dynamics that are smoothly changing with time. Details concerning the parameter selection are described in our previous publication [18].

C. New Approach for AF Detection: Variance of TVCF

For AF detection, we formulated two adjacent beat segments (RRI series) with the length denoted as seg using the following ARMA models:

$$S_{i+1:i+\text{seg}}\left(n\right)=-\sum_{i=1}^{P_1}g_1\left(n,i\right)S_{i+1:i+\text{seg}}\left(n-i\right)+\sum_{j=0}^{Q_1}h_1\left(n,j\right)S_{i+\text{seg}+1:i+2\cdot\text{seg}}\left(n-j\right)$$

$$S_{i+\text{seg}+1:i+2\cdot\text{seg}}\left(n\right)=-\sum_{i=1}^{P_1}g_2\left(n,i\right)S_{i+\text{seg}+1:i+2\cdot\text{seg}}\left(n-i\right)+\sum_{j=0}^{Q_1}h_2\left(n,j\right)S_{i+1:i+\text{seg}}\left(n-j\right) \quad (7)$$

where $S_{i+1:i+\text{seg}}\left(n\right)$ and $S_{i+\text{seg}+1:i+2\cdot\text{seg}}\left(n\right)$ are two adjacent RRI time series from the $(i+1)$th to the $(i+\text{seg})$th and from the $(i+\text{seg}+1)$th to the $(i+2\cdot\text{seg})$th, respectively. By substituting (7) into (6), the two transfer functions are obtained and the TVCF is obtained by the multiplication of the two TVCFs.

In order to illustrate AF detection, we calculated the TVCF using ARMA ($P_1=5$, $Q_1=5$) with the first order Legendre function for subject 8455 of the MIT-BIH AF database. We used the first order of Legendre polynomials as this choice resulted in the best accuracy for the MIT-BIH AF database ($N=23$). Further, use of one Legendre function resulted in poles to be within the unit circle, hence, all coherence values were bounded between 0 and 1. The optimal ARMA model order was found to be $P_1=5$ and $Q_1=5$ with $\text{seg}=128$, which will be explained in detail in the following section. We used a 128 beat segment, which was then shifted by 128 beats. We used a 64-point FFT, which resulted in a frequency resolution of 0.0156 Hz. Fig. 1 shows the resultant TVCFs according to each beat and normalized frequency (assuming a Nyquist frequency of 0.5 Hz). As shown in Fig. 1, the TVCF values are close to one throughout the entire frequency range for the two adjacent NSR data segments. However, the TVCF values significantly decreased when either or both segments partially or fully contained AF.

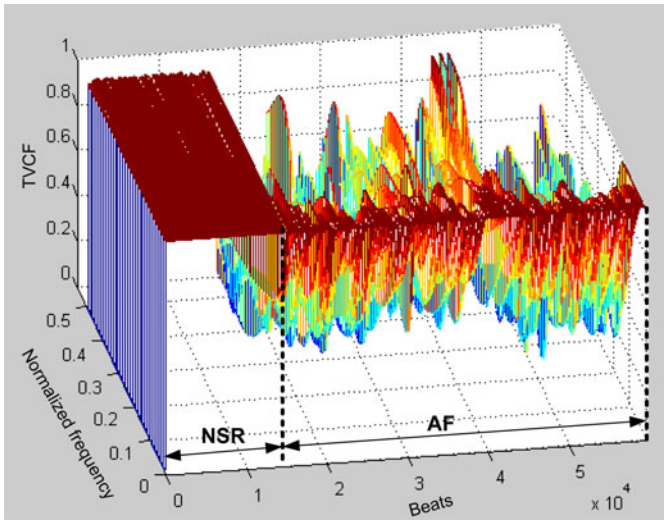

Fig. 1. Resultant TVCF of subject 8455 of the MIT-BIH AF database according to each beat and normalized frequency.

As shown in Fig. 1, we observe that the TVCF values are highly varying for different frequencies when the patient is in AF. That is, high frequencies tend to have lower coherence values than lower frequencies, in AF (see Fig. 2). To illustrate this phenomenon in more detail, we show some of the TVCF values selected at various frequencies from Fig. 1 as a function of time in Fig. 2(a). Fig. 2(b) shows the corresponding average values of TVCF according to each normalized frequency and each 128-beat segment for both the AF and NSR databases. We note that for AF data, TVCF values start close to one at low frequencies but they drop to low values quickly as the frequency increases. However, for NSR data, the TVCFs are nearly constant (slightly decreasing) at near unit values for all frequencies. This can be explained by the fact that the selected ARMA model terms for AF include largely self and its delay of one lag terms [e.g., *x(n), x(n–1), y(n),* and *y(n–1)*], as expected, thus, TVCF values will be high only at the low frequencies and decreases as frequencies increase. Our results for AF is expected since AF is known to have near random dynamics, hence, ARMA model parameters are limited to only low lag terms. Also note in the Fig. 2(a), we observe that the variance of TVCF values is significantly high for AF but nearly constant for NSR.

Based on the latter observation as described above, we propose AF detection by examining the variance of TVCF through the entire frequency range. For each beat, we calculate the variance of TVCF values, termed the frequency variations (FV),

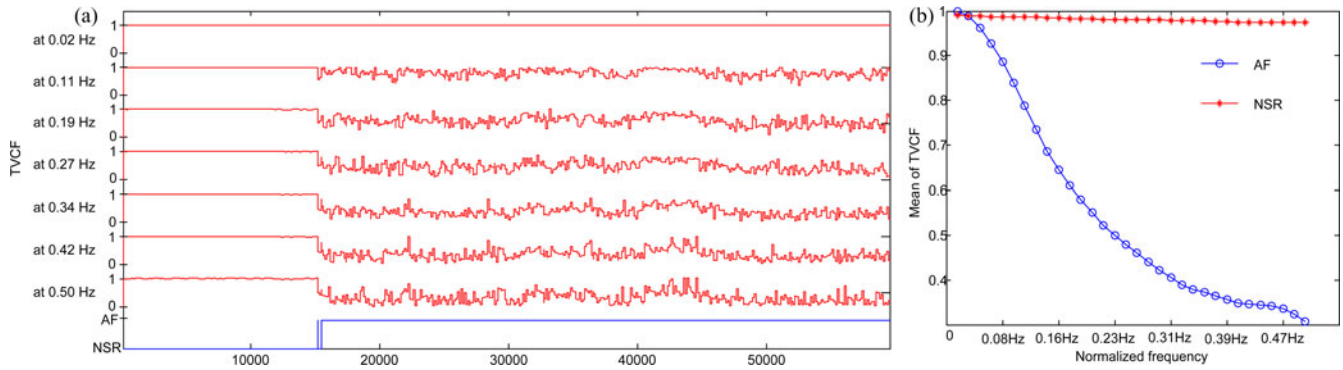

Fig. 2. TVCF at different frequencies with AF annotation and the mean of the TVCF with AF and NSR according to normalized frequency.

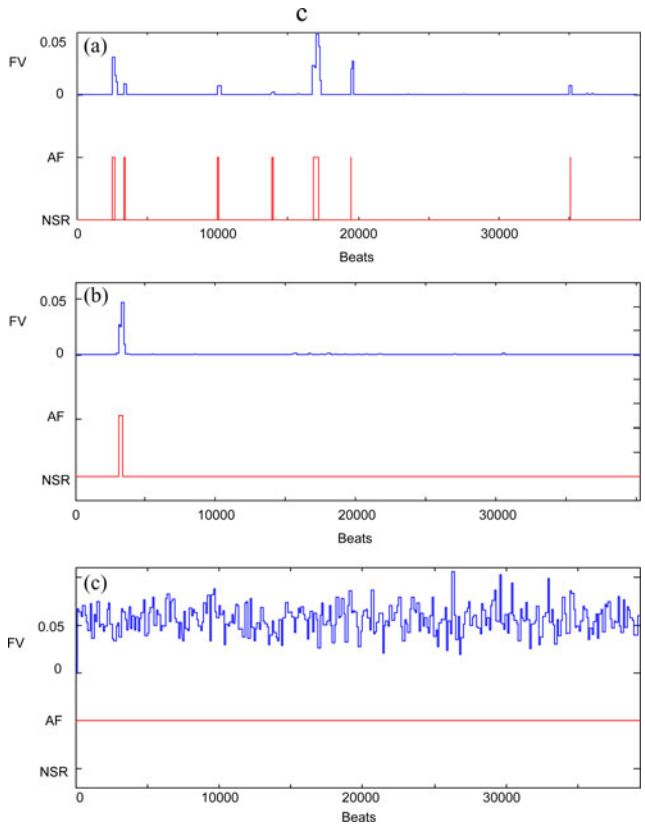

Fig. 3. True AF annotation; the values of FV. (a) MIT-BIH AF 4048. (b) MIT-BIH AF 735. (c) MIT-BIH AF 7162.

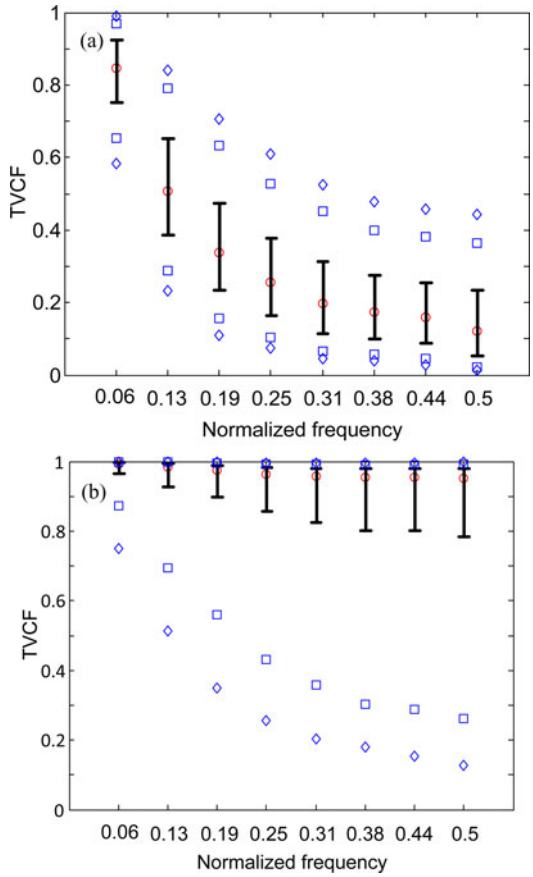

Fig. 4. TVCF value distribution of the entire MIT-BIH AF database according to each normalized frequency: (a) AF beats (b) NSR beats. The diamond above and below represent the 95th and the 5th percentiles of TVCF values according to each normalized frequency, and the square above and below represent the 90th and the 10th percentiles. Whiskers above and below represent the 75th and the 25th percentiles, respectively. The circle indicates the median value.

among all frequencies. Using FV-TVCF, we investigated the AF detection performance on the entire MIT-BIH AF database. Fig. 3 shows FV-TVCF values and true AF annotation for three representative subjects 4048, 735, and 7162 of the MIT-BIH AF database. In Fig. 3(a), the data set 4048 contains seven AF episodes with lengths of 206, 66, 37, 34, 388, 40, and 42 beats, and the values of FV-TVCF increase in the beats where AF occurs. In Figs. 3(b), the data set 735 contains one AF episode with a length of 332 beats whereas for the data set 7162 in Fig. 3(c), AF episodes persist for the entire time segment shown. The FV-TVCF values reflect this by never returning to a value of zero.

In Fig. 4, we show the distribution of TVCF value for the entire MIT-BIH AF database. Specifically, Fig. 4(a) and (b) shows the distribution of TVCF value for AF and NSR beats, respectively. The diamonds above and below represent the 95th and the 5th percentiles of TVCF values according to each normalized frequency, and the squares above and below represent the 90th and the 10th percentiles. Whiskers above and below

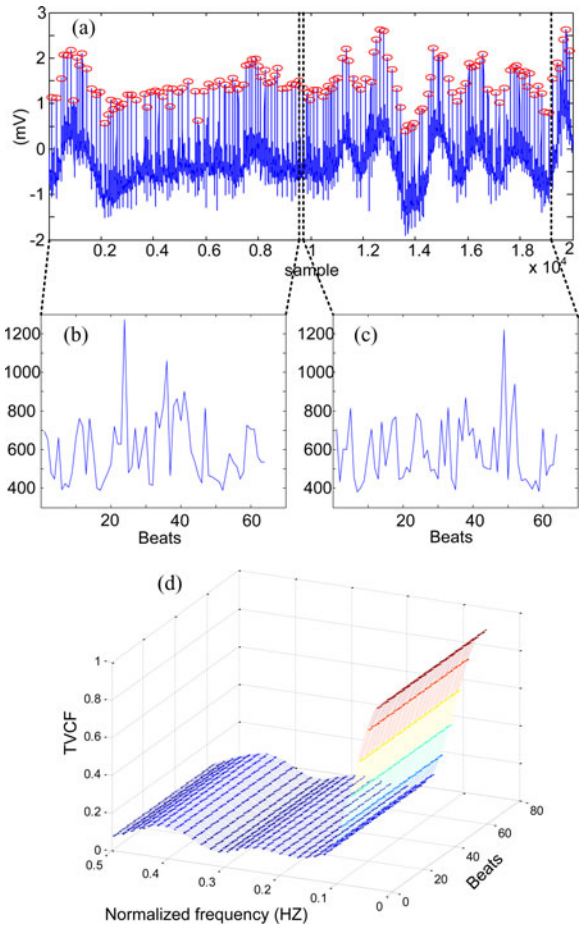

Fig. 5. Illustrative summary of TVCF for AF detection.

represent the 75th and the 25th percentiles, respectively. The circle indicates the median value.

Fig. 5 shows an illustrative summary of the procedures involved in the calculation of TVCF for AF detection. Fig. 5(a) shows an example of ECG signal from the data set 8455 of the MIT-BIH AF database. After R peaks have been determined, we calculate TVCF from the two adjacent beat segments (RRI series) as shown in Figs. 5(b) and (c), where in this case seg = 64. From the resultant TVCF, shown in Fig. 5(d), we then calculate FV-TVCF for the AF detection.

D. Ectopic Beat Elimination and Shannon Entropy Combination

A NSR segment including premature or ectopic beats may also result in lower TVCF values. In order to reduce the effect of the premature and ectopic beats, we eliminated outliers and filtered ectopic beats, as proposed in our earlier work [8]. To summarize, premature or ectopic beats can be recognized by their signature short-long RR sequence between normal RRIs. For each RRI in the time series, we computed the ratio *RR(i)/RR(i–1),* where *RR(i)* is the ith beat, and eliminated $RR(i)$ and $RR(i+1)$ when the following three conditions were satisfied: 1) $RR(i)/RR(i-1) < perc1$, 2) $RR(i+1)/RR(i) > perc99$ and 3) $RR(i+1)/RR(i+2) > perc25$, where *perc1*, *perc25*, *and perc99* are the 1st, 25th, and 99th percentiles based on a histogram of the RRI values, respectively. Note this strategy will remove some but not all complex arrhythmia patterns.

We also combined SE as in (8) with FV-TVCF, to increase the accuracy of AF detection. Specifically, the condition for AF detection is given by a simple logical AND condition

1 If (FV-TVCF $\geq \mathrm{TH_{var}}$) AND (SE $\geq \mathrm{TH_{SE}}$), then classify it as AF.
2 Else classify it as non-AF (NSR),

where $\mathrm{TH_{var}}$ and $\mathrm{TH_{SE}}$ are threshold values of FV-TVCF and SE, respectively.

SE has been shown to be a robust detector of AF [8] and is estimated according to the following calculation:

$$\mathrm{SE} = -\sum_{u=1}^{N_{\mathrm{bin}}} p(u) \frac{\log(p(u))}{\log\left(\frac{1}{N_{\mathrm{bin}}}\right)}. \tag{8}$$

Note that the optimal N_{bin} varies with the segment lengths. Hence, we also optimized the N_{bin} selection as well as the selection of the threshold parameters $\mathrm{TH_{var}}$ and $\mathrm{TH_{SE}}$ using the receiver operating characteristic (ROC) curves as detailed in the Section III.

III. Results

A. MIT-BIH AF Database

The top and bottom panels of Fig. 6 show the ROC curves with 1 minus specificity versus sensitivity for $\mathrm{TH_{var}}$ and $\mathrm{TH_{SE}}$, respectively, with seg = 128 and $P_1 = Q_1 = 5$. For the ROC evaluation, we found the number of True Positives (TP), True Negatives (TN), False Positives (FP), and False Negative (FN), and then calculated the sensitivity [TP/(TP+FN)], specificity [TN/(TN+FP)], and accuracy [(TP+TN)/(TP+TN+FP+FN)]. The best accuracy was found to be 0.9791 with $\mathrm{TH_{var}} = 0.019$ and $\mathrm{TH_{SE}} = 0.79$. We repeated the procedure by varying ARMA model orders from (2, 2) to (10, 10) and segment lengths from 12 to 128; the results are shown in Fig. 7. Seg = 128 provided the highest accuracy of all the segment length choices, but its result was not much different than with seg = 96. Interestingly, short segment lengths also provided high accuracy values (0.9222 with seg = 12 and 0.9421 with seg = 16). As for optimal ARMA model order, the accuracies were almost constant for (3,3) to (10,10) when seg = 128 or seg = 96. On the other hand, when seg = 12 or seg = 16, the order (2,2) provided the highest accuracy value. The detailed results for seg, (P_1,Q_1), accuracy, sensitivity, specificity, $\mathrm{TH_{var}}$, and $\mathrm{TH_{SE}}$ are shown in Table I. Using these optimal threshold values for seg = 128 [$\mathrm{TH_{var}} = 0.019$, $\mathrm{TH_{SE}} = 0.79$, *(p,q)* = (5,5)] and seg = 12 ($\mathrm{TH_{var}} = 0.000076$, $\mathrm{TH_{SE}} = 0.38$, *(p,q)* = (2,2), and seg = 12), we applied them to other databases (e.g., Arr, Holter data, and NSR). We are interested in short segment AF detection since 92.2% accuracy using only 12 beats is clinically significant as some of the paroxysmal AF episodes can be as short as 12 beats [22]. Table II shows sensitivity, specificity, and accuracy values with SE, FV-TVCF, and the combination of FV-TVCF with SE when seg = 12 and seg = 128. Comparisons to the recently published AF algorithms are presented in Table III. As

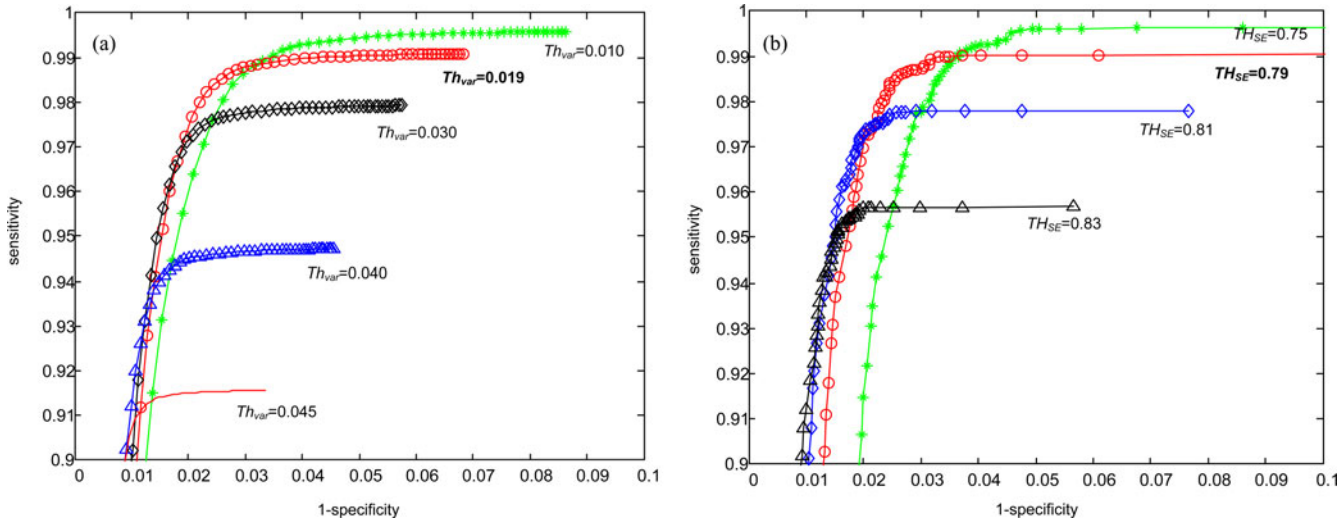

Fig. 6. ROC curves (1-specificity versus sensitivity) by changing $\mathrm{TH_{var}}$ from 0 to 0.1 and $\mathrm{TH_{SE}}$ from 0 to 0.1 where seg = 128, $p = q = 5$. (a) $\mathrm{TH_{var}}$=0.019 and (b) $\mathrm{TH_{SE}} = 0.79$.

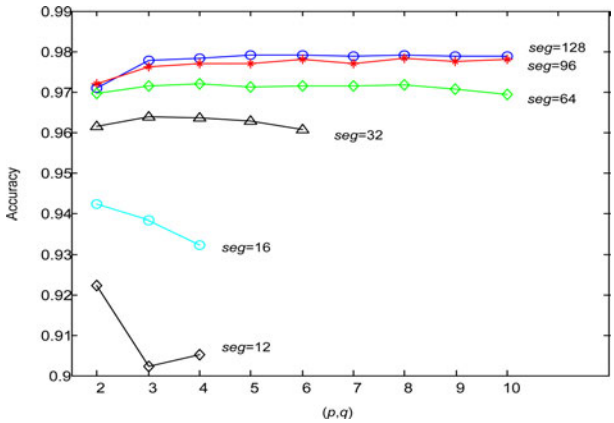

Fig. 7. Highest accuracy values according to model and segment length.

shown in Table III, our proposed algorithm provides the best accuracy for the MIT-BIH AF database. In addition, we found that the positive predictive values (PPVs) were 87.85% with seg = 12 and 96.89% with seg = 128.

Clinically, it is important to detect the presence of AF episodes in a given segment, not necessarily in every beat. Using this criterion on the MIT-BIH AF database (excluding files 4936 and 5091), the total number of true AF episodes is 255 and our algorithm with either seg = 12 or seg = 128 beats correctly detected the presence of all AF episodes. This result outperforms other recently published algorithms: 88.2% and 89.3% AF episode detection rate in Dash *et al*. [8] and Huang *et al*. [12], respectively. In addition, our algorithm provides one of the fastest transition times (e.g., AF to NSR or/and NSR to AF). Fig. 8 compares the transition time (delay beats). The median of the transition delay with seg = 12 is only six beats, which also outperforms any other recently published algorithm: 18 beats and 70 beats in Dash *et al*. [8] and Huang *et al*. [12]. Note that as the segment length decreases, the transition delay becomes better while the overall accuracy becomes worse.

It should be noted that in the MIT-BIH AF database, seven data sets excluding subject 4936 include 30 394 beats that have been classified as atrial flutter (AFL). Our method incorrectly detected only 1576 beats as AF out of 30 394 AFL beats (5.19%). It is possible that incorrect AF detection may be due to the fact that some of these AFL may have been classified as atypical forms of AFL, which have irregular RRI variability [23].

Fig. 9 shows the computation time according to seg and *(p,q)*, where the computation time is between 20 and 30 ms with seg = 128, and between 3 and 4 ms with seg = 12 (programs run in MATLAB 2010a on 2.66 GHz Intel Core2 processor). This shows that our algorithm can be realizable in real time for practical applications, and it is faster than other algorithms: 5.2 s with seg = 128 in Lake and Moorman [24], 200 ms with seg = 128 in Dash *et al*. [8], and 3 s with seg = 100 in Tateno and Glass [11].

B. MIT-BIH NSR Database, MIT-BIH Arr Database, and Clinical AF Database

We applied the optimal parameters mentioned above with seg = 12 and seg = 128 to the MIT-BIH NSR database, MIT-BIH Arr Database and Clinical AF Database. For the MIT-BIH NSR database the specificity was 94.37% with seg = 12 and 99.7% with seg = 128, which compares favorably to other published results: 99.7% with seg = 128 in Dash *et al*. [8], 97.9% with seg = 100 in Huang *et al*. [12], and 96.9% with seg = 500 in Kikillus *et al*. [9]. For the 100 series MIT-BIH Arr database, the specificity was 91.8% with seg = 12 and 99.7% with seg = 128, whereas it was 99.5% in Dash *et al*. [8] with seg = 128. Note that the 100 series contains no true AF beats. For the 200 series MIT-BIH Arr database, the sensitivity and specificity were 92.4% and 76.5% with seg = 12, and 91.1% and 89.7% with seg = 128 which compares well with 90.2% and 91.2% in Dash *et al*. [8] using seg = 128. In the 200 series MIT-BIH Arr database, the total number of true AF episodes is 79, and our algorithm with seg = 12 correctly detected 73 AF episodes

TABLE I
FV-TVCF WITH SE-BASED ACCURACY, SENSITIVITY, AND SPECIFICITY ARE LISTED WITH OPTIMUM THRESHOLD VALUES

seg = 128					
p,q)	Accuracy	Sensitivity	Specificity	TH_{var}	TH_{SE}
(2,2)	0.9709	0.9718	0.9703	0.0230	0.795
(3,3)	0.9779	0.9795	0.9766	0.0200	0.790
(4,4)	0.9782	0.9833	0.9744	0.0160	0.790
(5,5)	**0.9791**	**0.9822**	**0.9768**	**0.0190**	**0.790**
(6,6)	0.9790	0.9850	0.9746	0.0160	0.790
(7,7)	0.9787	0.9848	0.9742	0.0150	0.790
(8,8)	**0.9791**	**0.9815**	**0.9774**	**0.0220**	**0.790**
(9,9)	0.9788	0.9815	0.9768	0.0210	0.790
(10,10)	0.9787	0.9838	0.9750	0.0170	0.790

seg = 96					
(p,q)	Accuracy	Sensitivity	Specificity	TH_{var}	TH_{SE}
(2,2)	0.9719	0.9781	0.9672	0.1244	0.755
(3,3)	0.9763	0.9834	0.9711	0.0842	0.750
(4,4)	0.9768	0.9789	0.9753	0.1316	0.750
(5,5)	0.9769	0.9857	0.9703	0.0718	0.750
(6,6)	0.9781	0.9858	0.9724	0.0944	0.750
(7,7)	0.9770	0.9836	0.9721	0.1018	0.750
(8,8)	**0.9782**	**0.9848**	**0.9733**	**0.1036**	**0.750**
(9,9)	0.9774	0.9865	0.9707	0.0784	0.750
(10,10)	0.9780	0.9842	0.9734	0.1030	0.750

seg = 64					
(p,q)	Accuracy	Sensitivity	Specificity	TH_{var}	TH_{SE}
(2,2)	0.9695	0.9678	0.9708	0.0100	0.714
(3,3)	0.9715	0.9636	0.9774	0.0100	0.710
(4,4)	**0.9719**	**0.9654**	**0.9767**	**0.0100**	**0.710**
(5,5)	0.9711	0.9628	0.9771	0.0100	0.712
(6,6)	0.9713	0.9646	0.9763	0.0100	0.710
(7,7)	0.9714	0.9645	0.9765	0.0100	0.710
(8,8)	0.9717	0.9649	0.9767	0.0100	0.710
(9,9)	0.9706	0.9629	0.9763	0.0100	0.708
(10,10)	0.9695	0.9591	0.9771	0.0100	0.710

seg = 32					
(p,q)	Accuracy	Sensitivity	Specificity	TH_{var}	TH_{SE}
(2,2)	0.9614	0.9697	0.9553	0.0015	0.590
(3,3)	**0.9637**	**0.9668**	**0.9614**	**0.0010**	**0.590**
(4,4)	0.9635	0.9704	0.9584	0.0009	0.590
(5,5)	0.9629	0.9699	0.9577	0.0007	0.590
(6,6)	0.9607	0.9629	0.9590	0.0010	0.590

seg = 12					
(p,q)	Accuracy	Sensitivity	Specificity	TH_{var}	TH_{SE}
(2,2)	**0.9222**	**0.9474**	**0.9036**	**0.000076**	**0.380**
(3,3)	0.9021	0.8927	0.9091	0.000036	0.390
(4,4)	0.9051	0.9114	0.9003	0.000046	0.400

seg = 16					
(p,q)	Accuracy	Sensitivity	Specificity	TH_{var}	TH_{SE}
(2,2)	**0.9421**	**0.9481**	**0.9377**	**0.00033**	**0.480**
(3,3)	0.9382	0.9381	0.9383	0.00017	0.480
(4,4)	0.9323	0.9465	0.9218	0.00016	0.480

TABLE II
COMPARISON OF SENSITIVITY, SPECIFICITY, AND ACCURACY ON THE MIT-BIH AF DATABASE; SE, FV-TVCF, AND FV-TVCF WITH SE

	seg = 12			*seg = 128*		
	SE	TVCF	TVCF w/ SE	SE	TVCF	TVCF w/ SE
sensitivity	0.8285	0.9038	0.9474	0.9568	0.9558	0.9822
specificity	0.8639	0.9074	0.9036	0.9398	0.9556	0.9768
accuracy	0.8489	0.9124	0.9222	0.9471	0.9552	0.9791

TABLE III
COMPARISON OF RECENT ALGORITHMS ON THE MIT-BIH AF DATABASE AND THE MIT-BIH NSR DATABASE

Methods	MIT-BIH AF database		MIT-BIH NSR database
	sensitivity (%)	specificity (%)	specificity (%)
FV-TVCF	98.2	97.7	99.7
Dash et al [6]	94.4	95.1	99.7
Tateno and Glass [11]	94.4	97.2	*(not reported)*
Huang et al [12]	96.1	98.1	97.9
Logan and Healey [10]	96.0	89.0	*(not reported)*
Kikillus et al [9]	94.4	93.4	96.9
Lake et al [24]	91.0	94.0	*(not reported)*

(92.4%) which is better than the 73.4% in Dash *et al*. [8]. For the clinical AF database, the sensitivity and specificity were 93.9% and 84.4% with seg = 12, and 92.3% and 93.6% with seg = 128. Table IV summarizes the sensitivity and specificity values for SE, FV-TVCF, and the combination of FV-TVCF with SE when seg = 12 and seg = 128 based on MIT-BIH NSR, MIT-BIH Arr, and the Holter clinical databases. In addition, the PPVs were 45.17% with seg = 12 and 64.93% with seg = 128 for the MIT-BIH Arr 200 series. For the Holter clinical data, the PPVs were 90.51% with seg = 12 and 95.61% with seg = 128. Note

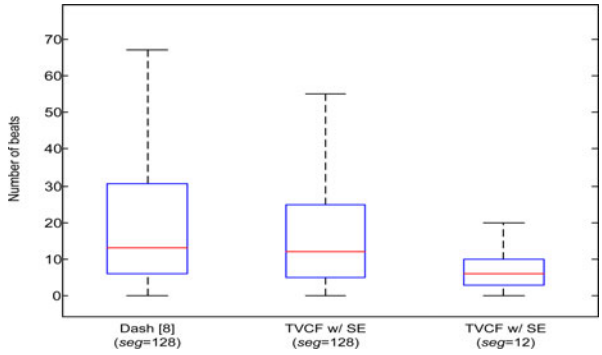

Fig. 8. Comparison of transition delay (beats).

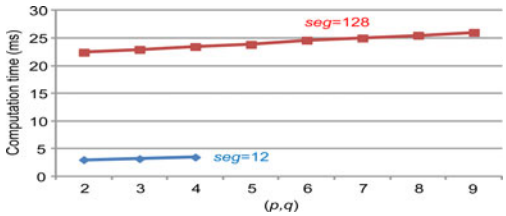

Fig. 9. Computation time according to seg and *(p,q)*.

TABLE IV
COMPARISON OF SENSITIVITY AND SPECIFICITY ON THE MIT-BIH NSR, ARR AND CLINICAL DATABASE: SE, FV-TVCF, AND RV-TVCF WITH SE

		seg = 12			seg = 128		
		SE	TVCF	TVCF w/ SE	SE	TVCF	TVCF w/ SE
MIT-BIH NSR	specificity	0.8212	0.9124	0.9437	0.8763	0.9888	0.9971
Arr (100)	specificity	0.7902	0.8843	0.9181	0.8316	0.9802	0.9965
Arr (200)	sensitivity	0.7996	0.8334	0.9242	0.8012	0.8592	0.9113
	specificity	0.7554	0.7742	0.7648	0.7942	0.8983	0.8968
Clinical	sensitivity	0.8481	0.8761	0.9387	0.8623	0.8847	0.9232
	specificity	0.7875	0.8452	0.8436	0.8012	0.8554	0.9364

that for the MIT-BIH Arr 200 series, the number of AF beats (9282 beats) is much smaller than the number of NSR beats (44 272 beats).

C. Smartphone Camera Data

We tested the algorithm with seg = 12, and obtained the sensitivity, specificity, and accuracy values of 91.40%, 93.93%, and 92.48%, respectively. These results show that highly accurate AF detection can be achieved with short duration data from a smartphone camera. With seg = 64, the sensitivity, specificity, and accuracy were found to be 97.16%, 95.39%, and 96.45%, respectively.

D. AF Surrogate Using White Noise

It is well accepted that dynamics of AF are random [25]. To examine if white noise dynamics has similar TVCF values as that of AF, we generated 128 000 samples from a normal distribution with mean 800 (ms) and standard deviation 30 (ms), and statically added varying levels of white Gaussian noise.

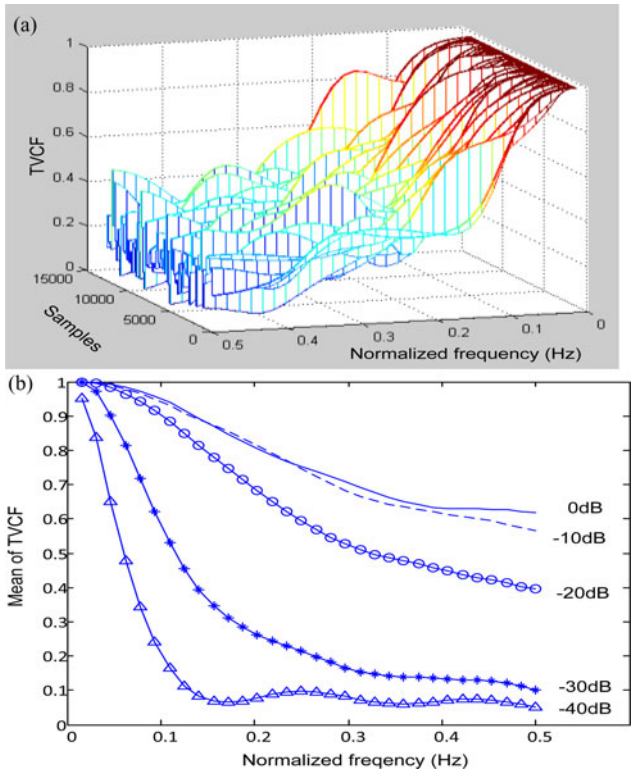

Fig. 10. TVCF of simulated white noise: (a) TVCFs of the signal with the –30 dB SNR according to each sample and normalized frequency, (b) Means of TVCFs according to normalized frequency and SNR.

The values of mean and standard deviation were selected to replicate the mean HR. The same ARMA model parameters for the calculation of TVCF on MIT-BIH databases were used: seg = 128 and $P_1 = Q_1 = 5$. Fig. 10(a) shows the TVCFs of the signal with the SNR of −30 dB for each of the 128 data segment. Similar to AF data [Figs. 1 and 2(b)], the TVCF values are close to one at zero frequency, and then decays quickly to low values with high degree of variability at high frequencies. Fig. 10(b) shows the average values of TVCF as a function of different SNR ranging from 0 to −40 dB. As expected, with the lowest SNR, the TVCF values are the lowest.

To examine if TVCF is also a better white noise detector than either the sample entropy or RMSSD, we show in Fig. 11simulation results based on varying levels of GWN. The rationale for this simulation is under the supposition that AF dynamics are similar to white noise. To each of the three plots, we provide AF detection threshold values for each of the method. The sample entropy and RMSSD/mean threshold values were set to −1.4 [24] and 0.1 [8], respectively, whereas the TVCF value of 0.019 was determined in the current study. As shown in Fig. 11, the sample entropy detects the white noise or AF when the SNR was –20 dB or lower. The RMSSD/mean could detect the white noise when the SNR was −25 dB or lower. On the other hand, FV-TVCF could detect the white noise when the SNR is either greater than or equal to −15 dB. Thus, the FV-TVCF is more a robust detector of white noise or AF since it has a wider dynamics range than either sample entropy or RMSSD approaches.

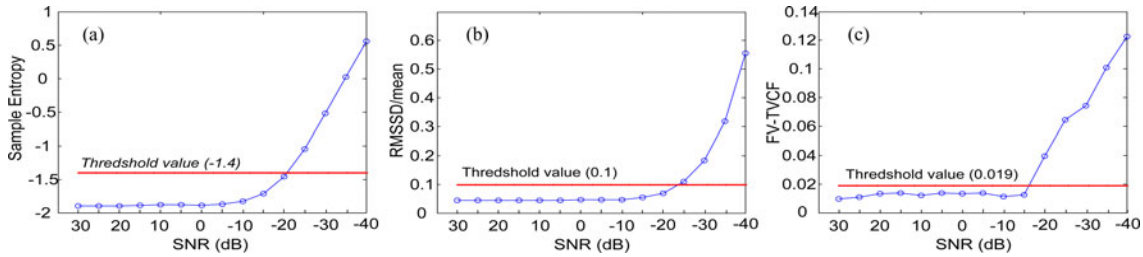

Fig. 11. Comparison of sample entropy, RMSSD/mean, and FV-TVCF for the white noise detection (a) Sample entropy, (b) RMSSD/mean, (c) FV-TVCF. For both RMSSD and sample entropy, any values above the defined threshold values are considered as AF detector whereas for TV-TVCF, it is below the defined threshold value of 0.019.

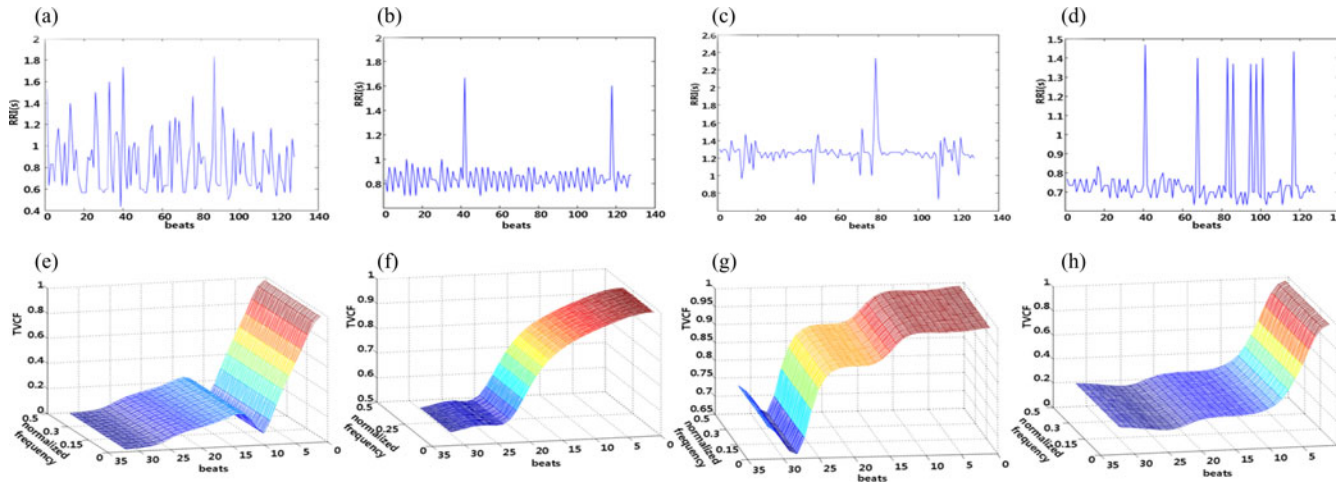

Fig. 12. Case study: TP (a,e), FN (b,f), TN (c,g), FP (d,h). Top panel shows RRI series and bottom panel shows FV-TVCF.

E. Ectopic Beat and Motion/Noise Artifact Elimination for the AF Detection Enhancement

We can increase the AF detection accuracy on all databases tested in this paper by eliminating ectopic beats albeit their presence was minimal especially for the MIT-BIH AF, NSR, and Arr 100 series data sets. The accuracy of AF detection on the MIT-BIH AF improved from 91.2% to 92.2% and from 97.1% to 97.9% with ectopic beat elimination when seg = 12 and seg = 128, respectively. For the MIT-BIH NSR, the accuracy improvement was negligible as ectopic beats were minimal. For the MIT-BIH Arr 100 series, the accuracy improved from 88.4% to 91.8% with seg = 12, and from 96.8% to 99.7% with seg = 128. For the MIT-BIH Arr 200 series, the accuracy improved from 72.4% to 79.2% with seg = 12, and from 78.6% to 89.9% with seg = 128. For the Holter clinical database, the accuracy improved from 89.9% to 90.1% with seg = 12 and from 92.4% to 92.9% with seg = 128.

Motion and noise artifact contamination is a significant problem for Holter recordings and they can result in false positive detection of AF. Indeed, some portions of Holter data were affected by motion and noise artifacts, and subsequently have led to incorrect R-wave peak location and AF detection. We recently developed the automatic motion and noise artifact detection in Holter ECG data [26], and used the algorithm for AF detection. Subsequently, by deleting the portions of data that were deemed to be contaminated with motion and noise artifacts, the specificity improved to 87.6% and 95.2% with seg = 12 and seg = 128, respectively. The increase in the sensitivity values was minor, however, for both data segment length.

F. Performance Analysis With Arrhythmias Other Than AF

In this study, the results from the MIT-BIH Arr 200 series and the clinical AF database show decreased specificity when compared to other databases (e.g., Arr 100), suggesting that the presence of many arrhythmias other than AF in these two databases are the culprit for the increased false positive rate. In order to investigate the effect of arrhythmias other than AF (e.g., premature atrial and ventricular contractions) on the accuracy of our algorithm, we further examined the specificity values of AF detection for both the MIT-BIH 200 series and Holter clinical data. For the MIT-BIH Arr 200 series, the specificity values were 94.4% for the NSR and 81.2% for the arrhythmias with seg = 128. For the Holter clinical database, the specificity values were 94.1% for the NSR and 86.3% for the arrhythmias with seg = 128. These results indicate that arrhythmias other than AF degrade the specificity of our algorithm due to increased false positive rates. Upon further examination of the reason for the decreased performance of our algorithm, what we found was that most of these data segments contained more than 50% arrhythmias other than AF. For example, of the 35 data segments from MIT-BIH Arr 200 series and 23 segments from the Holter clinical database with seg = 128 points, we found that 49 segments of these databases included more than 50%

arrhythmias (more than 64 beats). The remaining nine segments contained at least 25% arrhythmias. Hence, this suggests that our algorithm suffers in decreased specificity when arrhythmias other than AF are present for more than 50% of the data length. Certainly, the degradation of the specificity with our algorithm is to be expected since the TVCF is not specifically designed to discriminate other arrhythmias from the AF.

G. Additional Limitations

Fig. 12 shows the four cases of TP, FN, TN, and FP. The top panel shows RRI series and the bottom panel shows the corresponding FV-TVCF. The TP, FN, TN, and FP are shown in Fig. 12(a, e), (b, f), (c, g), and (d, h), respectively. As shown in Fig. 12(b), RRI randomness or high variability is not always associated with AF. This is the main limitation which affects most, if not all algorithms that look for RRI variability. In addition, as shown in Fig. 12(d), frequent ectopic beats may lead to a high false positive rate.

IV. Discussion and Conclusion

In this paper, we present a novel AF detection method by using an ARMA model-based approach to calculate the TVCF. The rationale for using the TVCF is twofold. First, AF dynamics are known to be highly random [8], [27], thus, the coherence function should be significantly lower than for NSR. Second, in cases of paroxysmal AF, AF dynamics are not only nonstationary, but they also transition frequently between NSR and AF. Indeed, Lovette and Roppella have applied the spectrogram approach to estimate TVCF and found that AF episodes have lower coherence values than NSR [15]. Note that because the aim of the study by Lovette and Ropella was not to detect AF episodes, their method's accuracy value was not reported [15]. Further, because the spectrogram does not provide the best time- and frequency resolution, its ability to find the transition between AF and NSRs is not as optimal as that of our high-resolution ARMA model-based TVCF [28]. Certainly, higher sampling rate can lead to improved results for the spectrogram but it may not be possible using certain recording device (e.g., smart phone) [29]. The dominant AF frequency is known to be time varying [30], thus, our use of TVCF is warranted. As noted in our previous development of the TVCF algorithm, the accuracy depends on the level of broadband characteristics of the signals. Certainly, AF which has random dynamics is well suited for the estimation of TVCF using our algorithm. Note also that NSR broadband characteristics [15], [31] make it well suited for the estimation by TVCF.

Utilizing our previously developed TVCF algorithm for AF detection, the AF detection accuracy was better than that reported in most previous studies [8]–[12]. Using our TVCF approach, the accuracy values with seg = 128 were 97.9%, 100%, 94.3%, and 92.2% on the MIT-BIH AF, the MIT-BIH NSR, the MIT-BIH Arr and clinical databases, respectively. While these accuracy values are noteworthy, the most attractive feature of the TVCF is that it can be used to accurately find AF onset and the transition to NSR since our approach provides good accuracy even with short data segments (seg = 12). This is important in order to accurately calculate AF burden, a measure of the percent of time a patient spends in AF.

Furthermore, our method is applicable for a Holter system as it is real-time realizable. The computation time was approximately 3–4 ms with seg = 12 and 20–30 ms with seg = 128 running MATLAB 2010a on a 2.80 GHz Intel Core2 processor. Real-time realizable capability is important not only for Holter monitoring, but also for AF detection using mobile devices [29]. We have recently shown that RRI data can be derived from a video camera that resides in a smart phone [29]. Given this new capability, AF detection is possible using a smart phone and the need for a real-time detection AF algorithm becomes even more evident.

References

[1] A. S. Go, E. M. Hylek, K. A. Phillips, Y. Chang, L. E. Henault, J. V. Selby, and D. E. Singer, "Prevalence of diagnosed atrial fibrillation in adults: National implications for rhythm management and stroke prevention: The AnTicoagulation and Risk Factors in Atrial Fibrillation (ATRIA) Study," *J. Amer. Med. Assoc*., vol. 285, no. 18, pp. 2370–5, May 2001.

[2] I. Hajjar and T. A. Kotchen, "Trends in prevalence, awareness, treatment, and control of hypertension in the United States, 1988–2000," *J. Amer. Med. Assoc*., vol. 290, no. 2, pp. 199–206, Jul. 2003.

[3] T. S. Tsang, G. W. Petty, M. E. Barnes, W. M. O'Fallon, K. R. Bailey, D. O. Wiebers, J. D. Sicks, T. J. Christianson, J. B. Seward, and B. J. Gersh, "The prevalence of atrial fibrillation in incident stroke cases and matched population controls in Rochester, Minnesota: Changes over three decades," *J Amer. Coll. Cardiol*., vol. 42, no. 1, pp. 93–100, Jul. 2003.

[4] M. Fukunami, T. Yamada, M. Ohmori, K. Kumagai, K. Umemoto, A. Sakai, N. Kondoh, T. Minamino, and N. Hoki, "Detection of patients at risk for paroxysmal atrial fibrillation during sinus rhythm by P wave-triggered signal-averaged electrocardiogram," *Circulation*, vol. 83, no. 1, pp. 162–9, Jan. 1991.

[5] G. Opolski, P. Scislo, J. Stanislawska, A. Gorecki, R. Steckiewicz, and A. Torbicki, "Detection of patients at risk for recurrence of atrial fibrillation after successful electrical cardioversion by signal-averaged P-wave ECG," *Int. J. Cardiol*., vol. 60, no. 2, pp. 181–5, Jul. 25, 1997.

[6] M. Budeus, M. Hennersdorf, C. Perings, and B. E. Strauer, "Detection of atrial late potentials with P wave signal averaged electrocardiogram among patients with paroxysmal atrial fibrillation," *Z. Kardiol*., vol. 92, no. 5, pp. 362–9, May 2003.

[7] D. Michalkiewicz, M. Dziuk, G. Kaminski, R. Olszewski, M. Cholewa, A. Cwetsch, and L. Markuszewski, "Detection of patients at risk for paroxysmal atrial fibrillation (PAF) by signal averaged P wave, standard ECG and echocardiography," *Pol. Merkur. Lekarski*., vol. 20, no. 115, pp. 69–72, Jan. 2006.

[8] S. Dash, K. H. Chon, S. Lu, and E. A. Raeder, "Automatic real time detection of atrial fibrillation," *Annu. Biomed. Eng*., vol. 37, no. 9, pp. 1701–9, Sep. 2009.

[9] N. Kikillus, G. Hammer, N. Lentz, F. Stockwald, and A. Bolz, "Three different algorithms for identifying patients suffering from atrial fibrillation during atrial fibrillation free phases of the ECG," *Comput. Cardiol*., vol. 34, pp. 801–804, 2007.

[10] B. Logan and J. Healey, "Robust detection of atrial fibrillation for a long term telemonitoring system," *Comput. Cardiol*., vol. 32, pp. 619–622, 2005.

[11] K. Tateno and L. Glass, "Automatic detection of atrial fibrillation using the coefficient of variation and density histograms of RR and deltaRR intervals," *Med. Biol. Eng. Comput*., vol. 39, no. 6, pp. 664–71, Nov. 2001.

[12] C. Huang, S. Ye, H. Chen, F. He, and Y. Tu, "A novel method for detection of the transition between atrial fibrillation and sinus rhythm," *IEEE Trans. Biomed. Eng*., vol. 58, no. 4, pp. 1113–9, Apr. 2011.

[13] H. Zhao, S. Lu, R. Zou, K. Ju, and K. H. Chon, "Estimation of time-varying coherence function using time-varying transfer functions," *Annu. Biomed. Eng*., vol. 33, no. 11, pp. 1582–94, Nov. 2005.

[14] L. S. Sarraf, J. A. Roth, and K. M. Ropella, "Differentiation of atrial rhythms from the electrocardiogram with coherence spectra," *J. Electrocardiol*., vol. 35, no. 1, pp. 59–67, Jan. 2002.

[15] E. G. Lovett and K. M. Ropella, "Time-frequency coherence analysis of atrial fibrillation termination during procainamide administration," *Annu. Biomed. Eng.*, vol. 25, no. 6, pp. 975–84, Nov.-Dec. 1997.
[16] S. L. Marple, *Digital Spectral Analysis With Applications*. Englewood Cliffs, NJ,, USA: Prentice-Hall, 1987.
[17] A. L. Goldberger, L. A. Amaral, L. Glass, J. M. Hausdorff, P. C. Ivanov, R. G. Mark, J. E. Mietus, G. B. Moody, C. K. Peng, and H. E. Stanley, "PhysioBank, PhysioToolkit, and PhysioNet: Components of a new research resource for complex physiologic signals," *Circulation*, vol. 101, no. 23, pp. E215–20, Jun. 2000.
[18] R. Zou, H. Wang, and K. H. Chon, "A robust time-varying identification algorithm using basis functions," *Annu. Biomed. Eng.*, vol. 31, no. 7, pp. 840–53, Jul./Aug. 2003.
[19] J. Lee and K. H. Chon, "Time-varying autoregressive model-based multiple modes particle filtering algorithm for respiratory rate extraction from pulse oximeter," *IEEE Trans. Biomed. Eng.*, vol. 58, no. 3, pp. 790–4, Mar. 2011.
[20] L. Faes, G. Nollo, and K. H. Chon, "Assessment of Granger causality by nonlinear model identification: Application to short-term cardiovascular variability," *Annu. Biomed. Eng.*, vol. 36, no. 3, pp. 381–95, Mar. 2008.
[21] X. Xiao, Y. Li, and R. Mukkamala, "A model order selection criterion with applications to cardio-respiratory-renal systems," *IEEE Trans. Biomed. Eng.*, vol. 52, no. 3, pp. 445–53, Mar. 2005.
[22] G. Y. Lip and F. L. Hee, "Paroxysmal atrial fibrillation," *QJM*, vol. 94, no. 12, pp. 665–78, Dec. 2001.
[23] D. E. Krummen, G. K. Feld, and S. M. Narayan, "Diagnostic accuracy of irregularly irregular RR intervals in separating atrial fibrillation from atrial flutter," *Amer. J. Cardiol.*, vol. 98, no. 2, pp. 209–14, Jul. 2006.
[24] D. E. Lake and J. R. Moorman, "Accurate estimation of entropy in very short physiological time series: The problem of atrial fibrillation detection in implanted ventricular devices," *Amer. J. Physiol. Heart Circ. Physiol.*, vol. 300, no. 1, pp. H319–25, Jan. 2011.
[25] M. A. Allessie, C. J. Kirchhof, K. T. Konings *et al.*, "Unravelling the electrical mysteries of atrial fibrillation," *Eur. Heart J.*, vol. 17, pp. 2–9, Jul. 1996.
[26] J. Lee, D. McManus, S. Merchant, and K. H. Chon, "Automatic motion and noise artifact detection in Holter ECG data using empirical mode decomposition and statistical approaches," *IEEE Trans. Biomed. Eng.*, vol. 59, no. 6, pp. 1499–506, Jun. 2012.
[27] K. M. Stein, J. Walden, N. Lippman, and B. B. Lerman, "Ventricular response in atrial fibrillation: Random or deterministic?," *Amer. J. Physiol.*, vol. 277, no. 2, pp. H452–8, Aug. 1999.
[28] S. Lu, K. H. Ju, and K. H. Chon, "A new algorithm for linear and nonlinear ARMA model parameter estimation using affine geometry," *IEEE Trans. Biomed. Eng.*, vol. 48, no. 10, pp. 1116–24, Oct. 2001.
[29] C. G. Scully, J. Lee, J. Meyer, A. M. Gorback, D. Granquist-Fraser, and K. H. Chon, "Physiological parameter monitoring from optical recordings with a mobile phone," *IEEE Trans. Biomed. Eng.*, vol. 59, no. 2, pp. 303–6, Feb. 2012.
[30] R. Alcaraz, F. Sandberg, L. Sornmo, and J. J. Rieta, "Classification of paroxysmal and persistent atrial fibrillation in ambulatory ECG recordings," *IEEE Trans. Biomed. Eng.*, vol. 58, no. 5, pp. 1441–9, May 2011.
[31] K. H. Chon, Y. M. Chen, N. H. Holstein-Rathlou, and V. Z. Marmarelis, "Nonlinear system analysis of renal autoregulation in normotensive and hypertensive rats," *IEEE Trans. Biomed. Eng.*, vol. 45, no. 3, pp. 342–53, Mar. 1998.
[32] J. Lee, D. McManus, and K. Chon, "Atrial fibrillation detection using time-varying coherence function and Shannon entropy," in *Proc. IEEE Conf. Eng. Med. Biol. Soc.*, 2011, pp. 4685–8.

Authors' photographs and biographies not available at the time of publication.